DUAL-FREQUENCY IP[1]

He, Jishan
Department of Geology, Central South University of Technology, Changsha 410083, China

ABSTRACT

The dual-frequency (DF) IP is a new kind of frequency domain IP method. Not only is the dual-frequency current transmitted simultaneously but the electric potential difference due to dual frequency current is measured synchronously. This paper discusses the principle and charateristic of DF current , DF current can be formed by two rectangular currents which must be coherent or else false Percent Frequency Effect (PEE) will occur. DF currents with different waveforms are equivalent in the ability of detecting IP anomalies. Unstable current has much less effect of DF IP than on conventional variable frequency method; in fact, there is no need to stabilize current in DF IP method. There are many differences between harmonic contents of DF current and that of rectangular wave used in variable frequency method, but theoretical analysis, labaratory modeling and field data all show that the anomalies of both DF and variable frequency method are similar in character and close in value. DF IP can match variable frequency IP and time domain IP in the ability of detecting IP anomaly, furthermore, dual-frequency IP measurements are more rapid, more accurate and more simple in operation.

Key words: dual frequency IP percent frequency effect IP anomaly

1 INTRODUCTION

In the fall of 1950, Wait, J R successfully made a frequency-domain IP experiment in Arizona[1]. He measured IP effect by varying the frequency, and published his famous paper, i. e. "Variable-frequency method". In 1960s, Macphar Co. produced transmitter of P-550 which suplies two frequencies simultaneously, but the receiver still measures them in turn. Then, The occurrence of IPRF-2 made use of harmonics in frequency domain IP method. Zonge, K L developed and improved harmonics method and held the parent of harmonics compler resistivity[2]. Pelton, W H put forward spectral IP of measuring multi-frequency phase in turn[3].

IP method, as an effective technique of searching metallic ores, has been used in China more than 30 years. However, frequency-domain IP was used in practice in 1970s[1]. The author had been systematically investigating "Dual-frequency IP method" since 1970s. Besides theoretical research, the author has developed a new kind of equipment, DUAL-FREQUENCY IP SYSTEM, that has been used successfully in 24 provinces in China so far, and many metallic ores and groundwater sources have been found with this system.

The main idea of dual-frequency IP is that not only does the transmitter apply the coherent currents with two frequencies simul-

① Manuscript received Sept. 24, 1993

taneously; but also the receiver measures the signals with these two frequencies simultaneously. In reconnaissance, a pair of frequencies for example 4/13 Hz and 4 Hz, is used or only the amplitudes of potential difference due to this pair of frequencies current are measured to calculate Percent Frequency Effect (PFE), or amplitudes and phases/real and imaginary components of potential differences of this dual-frequency are measured. If necessary, spectral IP measurements can be done by transmitting several pairs of frequencies in sequence.

2 WAVEFORMS OF DUAL-FREQUENCY CURRENT

Although various kinds of dual-frequency current formations are available, it is an ideal condition when high frequency (HF) and low frequency (LF) current are completely coherent. The complete coherence means that both HF and LF current remain a constant relationship between their amplitudes, frequencies, and phases. f_h, f_l, ω_h and ω_l are used to represent the frequencies and angular frequencies of HF and LF currents respectively, $s = f_h/f_l$ represents coefficient of frequency difference between HF and LF currents, $\delta\omega_h$ the phase shift of the fundamental of HF current relative to the s th-order harmonic of LF current.

When HF and LF current are rectangular waves with same amplitudes, the waveform of dual-frequency is only dependent on s and $\delta\omega_h$. Fig. 1(a) and 1(f) show the general current waveforms of dual-frequency current with odd s and even s respectively, whose expanded forms are as follows:

$$I(t) = \frac{4I_0}{\pi}\sum_{k=1}^{\infty}\frac{1}{2k-1}[\sin(2k-1)\omega_l t + \sin(2k-1)s\omega_l(t-\delta\omega_h)] \quad (1)$$

For convenience, $\delta\omega_h$ are given with some special values. For example, $\delta\omega_h = 0$ (Fig. 1(b)), i.e. the fundamental of HF current has the same phase as that of the s th-order harmonic of LF current. Expanding dual-frequency current into a Fourier series, the amplitude of the k th-order current is expressed as

$$I_k = [1-(-1)^k]\frac{I_0}{k\pi} \times \left[2 - \frac{\sin\frac{(s-1)k\pi}{2s}\cdot\sin\frac{k\pi}{2}}{\cos\frac{k\pi}{2s}}\right] \quad (2)$$

at this point, the ratio of the amplitude of HF current to that of LF current is $I_h/I_l = 1 + 1/s$.

When $\delta\omega_h = \pi$ (Fig. 1(c)), the amplitude of k th-order is

$$I_k = [1-(-1)^k]\frac{I_0}{k\pi}\sin\frac{(s-1)k\pi}{2s} \times \sin\frac{k\pi}{2}/\cos\frac{k\pi}{2s} \quad (3)$$

and $I_h/I_l = 1 - 1/s$ due to the fundamental of HF current possessing a phase opposite to that of the s th-order harmonic of LF current.

Fig. 1(d) and 1(e) show the waveforms at $\delta\omega_h = \pm\pi/2$ respectively. They can be written as

$$I(t) = \frac{4I_0}{\pi}\sum_{k=1}^{\infty}\frac{1}{2k-1}[\sin(2k-1)\omega_l t \pm \cos(2k-1)s\omega_l t] \quad (4)$$

This means the fundamental of HF current is orthogonal to the s th-order harmonic of LF current.

Fig. 1(g) ~ 1(j) show the current waveforms for $\delta\omega_h = 0, \pi$ and $\pm\pi/2$ respectively when s is even. The situation is similar to the above, but two points are noteworthy. First, the fundamentals of HF and LF currents are equal no matter whatever values of $\delta\omega_h$ may be. Second, no difference will take place for the application of the cur-

rent waveforms when the $\delta\omega_h$ takes anyone of the four values: 0, π or $\pm\pi/2$.

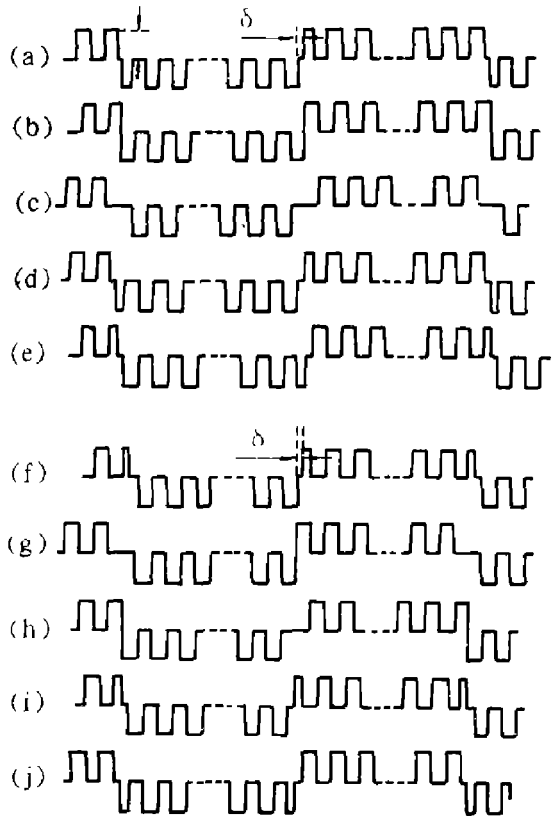

Fig. 1 Summary of dual-frequency current waveforms δ-phase lag between high and low frequencies

Something may be seen from the above analysis of waveforms.

(1) The magnitude of $\delta\omega_h$ has notable effect on the constituents of HF and LF currents, therefore, $\delta\omega_h$ has to be remained constant otherwise the change of $\delta\omega_h$ will lead to notably false PFE. If dual-frequency current is formed by HF and LF currents from different sources, the phase difference between them will be random. For example, for a given measurement, $\delta\omega_h = 0$, and for another, $\delta\omega_h = \pi$, false Percent Frequency Effect $P_f = 2/(s+1)$ can be obtained from expressions (2) and (3). At $s = 13$, P_f is up to 14.3%. Such a large P_f is unpermitted; therefore, it is neccessary for the dual-frequency current to be coherent.

(2) with regard to practical applications, the above waveforms, each has its own features can be used according to different requirements, but they are equivalent in detecting IP anomaly

Fig. 2 shows the model experiments of two current waveforms on resistance-capacitance (RC) network. The RC simulating is to remain simulated object stable, so that only the difference due to different waveforms can be picked out. Here, $f_1 = 0.3$ Hz, $s = 13$ and $\delta\omega_h = 0$ and π respectively. Fig. 2 shows clearly that two curves are nearly overlapped, the relative error is only 1.3%.

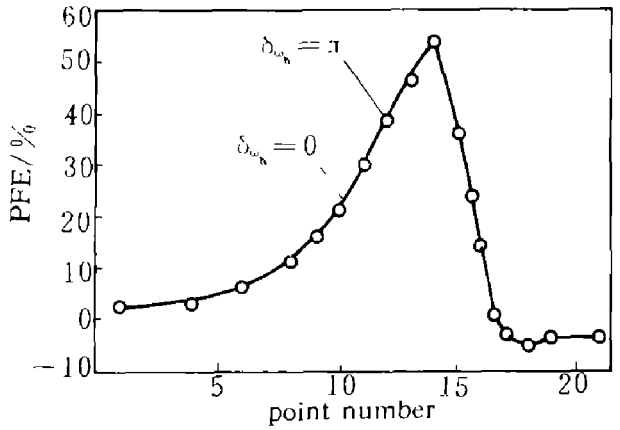

Fig. 2 Percent frequency effect measured on a R-C model with different dual-frequency current waveforms

Figs. 3 and 4 show the results field measurements of different current waveforms. The anomalies due to pyrite over a limestone zone of weathering at Mountain Heng, Hunan, China, are observed from Fig. 3, of which curve 1 and curve 2 present the measurements with DF IP system and with Canada Huntec Marx-Ⅲ time-domain receiver respectively. The parameters of DF current are $f_1 = 0.3$ Hz, $s = 13$, $\delta\omega_h = \pi$. Fig. 4 shows the measurements over a molybdenum mine, the parameters of DF current are $f_1 = 0.3$ Hz, $s = 13$, $\delta\omega_h = 0$. The dual-fre-

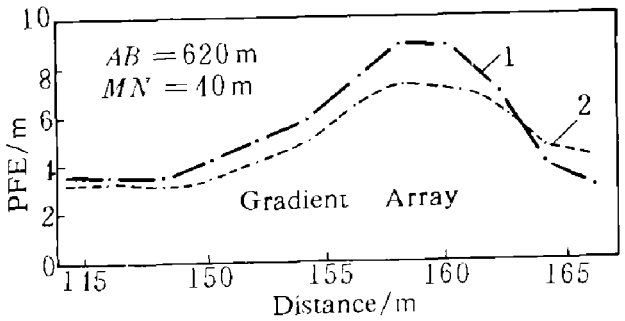

Fig. 3 Comparison of IP profiles

(1)—measured with the DSF—79 Dual Frequency IP Equipment, current parameters: $s = 13$, $\delta\omega_h = \pi$, $f_1 = 0.3$ Hz;
(2)—measured with the Huntec Mark-Ⅲ time-domain receiver

quency anomaly PFE is in good agree-ment with TD IP anomaly, and the former has a more smooth curve than that of the latter because of the higher measuring precision.

From above model experiments and field measurements, it is very obvious that the different current waveforms are equivalent in showing IP anomaly.

3 THE EFFECT OF CURRENT VARIATIONS

In the conventional variable frequency method, the HF and LF currents are supplied at different time and then the relevant potential is measured. The current variation directly brings about false PFE, so that current has to be stabilized. But it is different in DF IP method in which the current of two frequencies are injected into the ground simultaneously so that the effect of current variation is much less.

The current variations can be divided into three categories: First, the apparent frequency of current variation is lower than f_1 of LF. For example, if the current applied by the transmitter is unstablized, the current variation due to the gradual fall of power volt-age or gradual variation of earth resistance of the current-applying electrodes belong to the first sort . Second, varying ap-

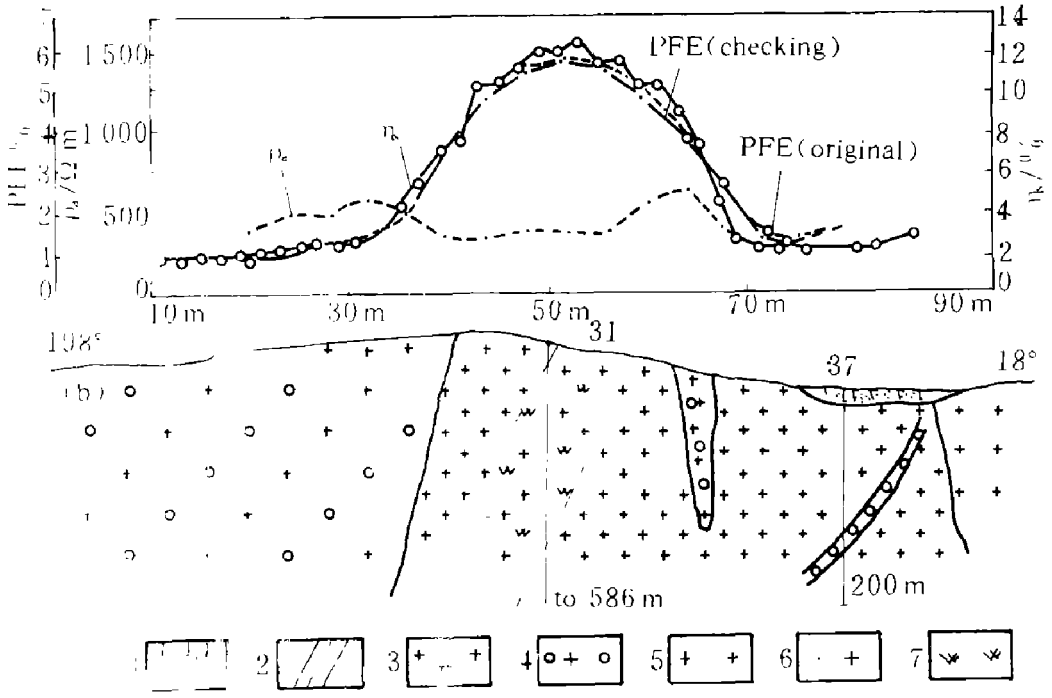

Fig. 4 Comparison of IP profiles

(a)—measured with the DSF-79 Dual Frequency IP Equipment, current parameters: $s = 13$, $\delta\omega_h = 0$, $f_1 = 0.3$ Hz; (b)—time domain IP response
1—quaternary system; 2—fractured zone; 3—granite; 4—granitic breccia; 5—granite-porphyry; 6—quartz-porphyry; 7—pyritization

parent frequency is higher than f_h. In a sense, this sort can be further divided into two--one belongs to periodically systematic variation, the other transient pulse variation. When AC current is rectified and is used as power source, its residual ripple belongs to the former, and the generator rotation speed variation or other electrical interference belong to the latter. Third, the apparent frequency varies between f_l and f_h. The effects of three on measurements are similar to that of earth noise. Here, only the first and third categories will be expounded, and the second will be discussed in the paper on the anti-interference ability of dual-frequency method.

Fig. 5 shows the first and third categories of current variation curves which can be used to calculate the effect of current unsteadiness on PFE. In the first one , as shown in Fig. 5(a), assuming the envelop amplitude varies with time according to the following equation:

$$|I(t)| = |I_0 - \beta t|$$

during the current-applying time, $|I_0| \geqslant |\beta t|$. To make the expressions of calcula-

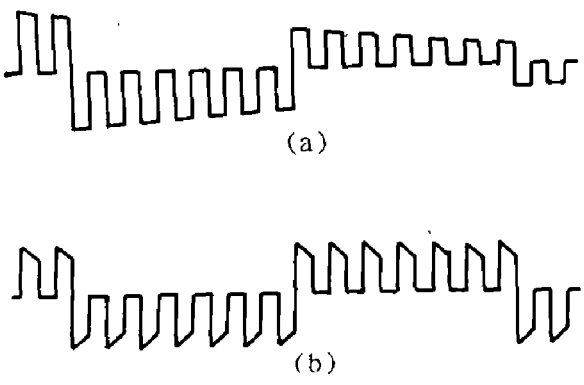

Fig. 5 Unsteady dual-frequency current waveforms for calculation of the effect of current unsteadiness on IP response

tions more simple but not to reduce the generality of the question discussed, the variable apparent frequency is assumed to be f_1/s.

This linearly variable dual-frequency current can be expanded into Fourier series. The amplitude of the k th-order harmonic is

$$I_k = \frac{1}{k\pi}\{4\pi\beta + (2I_0 + \frac{\beta\pi}{s}) \cdot \sin k\pi \times \sin\frac{(2s+1)k\pi}{2s}/\cos\frac{k\pi}{2s} + \frac{2\beta}{k} \times \sin k\pi \cdot \cos(\frac{2s+1}{2} \cdot \frac{k\pi}{s})/\cos\frac{k\pi}{2s} - \frac{4\beta\pi}{s} \cdot 2s\cos\frac{k\pi}{2s}\cos\frac{(4s+1)k\pi}{2s} \div (1+\cos\frac{k\pi}{s})\} \quad (5)$$

The relative error of LF voltage due to the current variation is

$$\Delta U_1/U_1 = \beta\pi/(2sI_0)$$

the consequent false PFE is

$$P_f = -\beta\pi/(sI_0)$$

Obviously, this variation has little effect on the measurements of PFE, which is a great advantage of the dual-frequency method. For example, the voltage of power-source decreases with time so that the current intensity decreases by 20% within 45s. In this condition, the conventional variable frequency will introduce 20% false PFE, making it impossible to work. Even if the current is stabilized with a precision about 0.5%, about 1% false PFE will be introduced, which is unpermitted. But, in the same condition, even the current is not stabilized, the dual-frequency method only brings about 0.1% false PFE.

The third effect is discussed with model in Fig. 5(b). The DF current is on and off at each LF semi-period due to HF modulation. If battery voltage variation, earthing resistance variation or other effects cause the current to vary linearly, when the current is on, and recovers its original condition, when the current is off, it behaves as shown in Fig. 5(b). (s is an odd, $\delta\omega_h = \pi$). then, we have

$$I_k = \frac{1-(-1)^k}{k\pi}\{2I_0 - I_0 \times \sin\frac{(s-1)k\pi}{2s} \cdot \sin\frac{k\pi}{2}/\cos\frac{k\pi}{2s} + \frac{\beta\pi}{s} \times \sin\frac{(s+1)k\pi}{2s}/(2\sin\frac{k\pi}{s}) + \frac{\beta}{k} \times \sin\frac{(s-1)k\pi}{2s}\cos\frac{k\pi}{2s}/\cos\frac{k\pi}{2s}\} \quad (6)$$

the relative error of LF voltage due to current variation and the corresponding false PFE (P_f) equals 0. If $s = 13$, $f_1 = 0.3$ Hz, and the rate of current variation is 1% per second, $\triangle U_1/U_1$ is only 0.13%, and $P_f = 0$, therefore, it hardly has effect on PFE. To examine the effect of the current variation on PFE, a series of model experiments have been made.

Fig. 6(a) shows that if the current reduces by 38% in 480 s, i.e. by 3.5% in the time of s/f_1, the consequent P_f is 0.0 to 0.3%. In conventional variable frequency method, a P_f of several percentage points will be caused under such a large current variation, but the exact value depends on the time difference between HF and LF measuring time. For example, if the time difference is 47 s, the error should be as high as 3.5%, and obviously, it is impossible to work. Fig. 6(b) and 6(c) present data from two sets of experiments under faster current variation condition, in the time of s/f_1, the current variations are 7% and 24%, and the relevant false PFE are 0 to 0.4% and 0 to 0.6% repespectively. Fig. 6(d) shows the effect of current variation in the present of anomaly. It can be seen that with a current variation up to 60%, the relative variation of anomaly is only 2%. In these experiments, large current variations were used for emphasizing the effect of current variation on PFE.

The above calculations and experiments were made assuming the power voltage varies linearly. If the voltage of power source varies at slow rate, it will be considered linear for a given time. Therefore, in dual-frequency method unstablized current

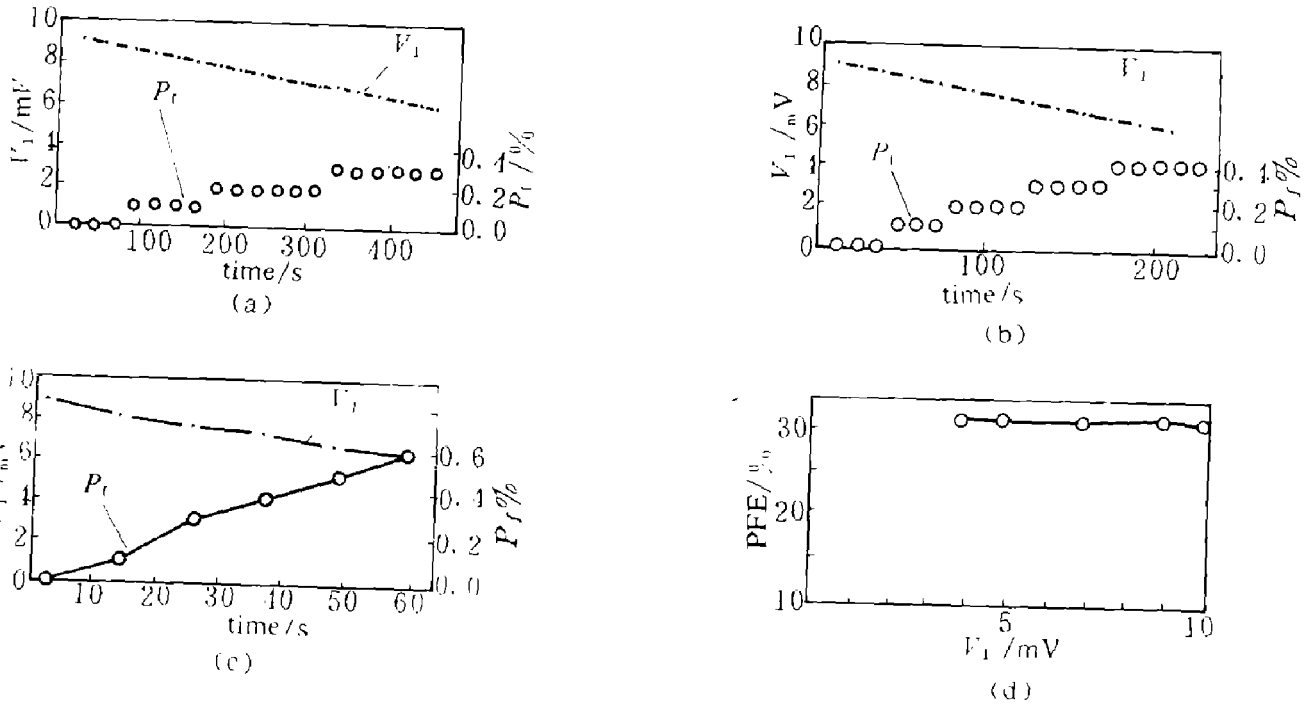

Fig. 6 Variation of Percent Frequency Effect PFE function of current unsteadiness

can be used if the power voltage variation is nearly linear. In fact, the unstabilized current was used in the applications of dual-frequency method in Gangshu and Hei Longjiang provinces, China. Fig. 7 shows quality examinations of the method at an area in Gangshu. The original observation preceded the exam observation for 4 days; unstabilized current was used in both observations, so there is a good agreement between the two curves. Also, unstabilized current used in Hei Longjiang is shown in Fig. 4, and good agreement has been achieved. These results have proved that unstabilized current can be used in dual-frequency method, with which power utilization can be increased, transmission can be simplified and its stability can be improved.

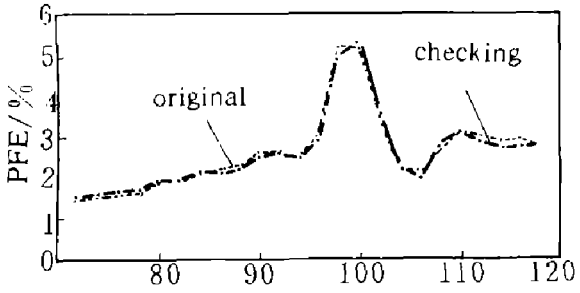

Fig. 7 IP profiles measured with DSF-79 Dual Frequency IP Equipment using unstabilized dual-frequency current

4 ANOMALIES OF DUAL-FREQUENCY IP

In conventional variable frequency method, the current applied is a simple rectangular wave whose frequency is the same as that of the corresponding current and the high-order harmonics attenuate with the orders, i. e.

$$I(t) = \frac{4I_0}{\pi}\sum_{k=1}^{\infty}\frac{1}{2k-1}\sin(2k-1)\omega t \quad (7)$$

where I_0 is the amplitude of the rectangular current; ω is the angular frequency. After current passes through the corresponding bandpass filter, the high-order harmonics of the potential difference are reduced greatly; hence the quasi-sine-wave with corresponding frequency is obtained, no matter HF or LF potential is measured.

But the situation is different in the dual-frequency IP survey. Transmitter applies dual-frequency current $I_s(t)$ whose amplitude of HF/LF current is

$$I_s(t) = \frac{4I_0}{\pi}\sum_{k=1}^{\infty}\frac{1}{2k-1}[\sin(2k-1)\omega_l t + \sin(2k-1)(\omega_h t - \delta\omega_h)] \quad (8)$$

where ω_l, ω_h are the angular frequency of LF and HF currents respectively; $\delta\omega_h$ is the phase difference between the s-order harmonic of LF retangular wave and the fundamental of HF; $s = \omega_h/\omega_l$. At low frequency, dual-frequency method is similar to the conventional variable frequency method due to the frequency of the fundamental being same as the low frequency. But some high order harmonics of LF current, the frequency of which are same as or close to the frequency of HF current, will certainly have effect on the HF current because of simultaneous exsistence of high-and low frequency, therefore, to this effect attention must be paid.

There should be suitable width of HF and LF channels in any receivers; a width too wide will reduce the anti-interference ability, and a width too narrow will prolong the transient. The authors designed the relative bandwidth of high and low channel at 0. 9 so that the harmonics from orders 7 to 19 of LF current are in the range of HF channels . Part of harmonics contribute to the output of HF channel that are beyond the band, especially those harmonics of lower frequencies. The effects are analyzed by following model:

$$U_h(t) = \frac{2}{\pi}\sum_{k=1}\frac{1}{2k-1}[A_l B_l \sin(2k-1)\omega_l t$$

$$+ A_2B_2\sin(2k-1)\omega_h(t-\delta)] \quad (9)$$

$$U_l(t) = \frac{2}{\pi}\sum_{k=1}^{\infty}\frac{A_1B_2}{2k-1}\sin(2k-1)\omega_l t \quad (10)$$

where

$$A_1 = 1 - k_s\lg[(2k-1)f_l]$$
$$A_2 = 1 - k_s\lg[(2k-1)f_h]$$
$$B_1 = (1-a)[\frac{a(2k-1)^4}{s^4} - 2\frac{a(a+1)(2k-1)^2}{s^2} + 5a^2 + 1 - \frac{2a(a+1)s^2}{(2k-1)^2} + \frac{as^4}{(2k-1)^4}]^{-1/2}$$

B_2 is the B_1 when $s=1$, where $U_h(t)$ and $U_l(t)$ are the voltage outputs of HF and LF filters respectively. A_1 and A_2 are parameters simulating the IP response from earth, that is to assume the apparent resistivity possesses a linear relation to the logarythm of frequency. k_s is the linear coefficient. B_1 and B_2 simulate the low-pass and high-pass characteristics of frequency respectively, a is a constant related to the values of bandpass Q as follows:

$$a = 1.39e^{-1.76/Q} \quad (11)$$

V_l and V_h represent DC voltage outputs of averages of low-pass and high-pass having been detected, i.e.

$$V_h = \int_0^{1/f_l}|U_h(t)|dt,$$
$$V_l = \int_0^{1/f_l}|U_l(t)|dt \quad (12)$$

hence

$$\text{PFE} = (V_l - V_h)/V_h \quad (13)$$

The effect due to varying values of the quantities K, Q and s was calculated, from the calculations several conclusions can be made as follows:

(1) The output of LF channel filter is shaped as a quasi-sine wave which is between sine wave and square wave and is more close to sine wave (Fig. 8(a) and 8(b)). Comparing the curve 8(a) with curve 8(b), it is obvious that more narrow is the relevant bandpass, more close is the shape of quasi-sine wave to that of sine wave.

(2) The waveform of high-pass voltage differs somehow from that of sine wave. From the waveforms shown in Fig. 8, it may be seen that on the basis of quasi-sine vibration, additional vibrations take place whose apparent frequency is the same as that of low frequency; and it causes an increase of amplitude at $\delta\omega_h = 0$ and a decrease of amplitude at $\delta\omega_h = \pi$. All those are caused by LF harmonics, especially by those close to high frequency. The shape of total highpass output is also more close to sine wave.

(3) The variation of the shape of passband will bring about the variation of the constituents of harmonics. Obviously, PFE is different with different bands and constituents of harmonics. The bandpass shapes of receiver have effect on PFE measurements but very little effect in general cases (i.e. $Q > 1$). PFE measured with DF method is very close to that with variable frequency method. They have equivalent ability of discovering IP phenomenon.

To verify the above conclusions, systematic model experiments have been made in RC network with the No. 1 receiver whose HF and LF passes have similar frequency characteristic curves; the value of Q of HF pass is 1.05, and that of LF pass is 1.43. The measurements are shown in Table. 1. Calculations in Table. 1 are made with sine waves of frequencies 0.3 and 3.9 Hz respectively, i.e. they are the results of conventional variable frequency method under ideal condition. From Table. 1, it may be seen that the absolute error between the

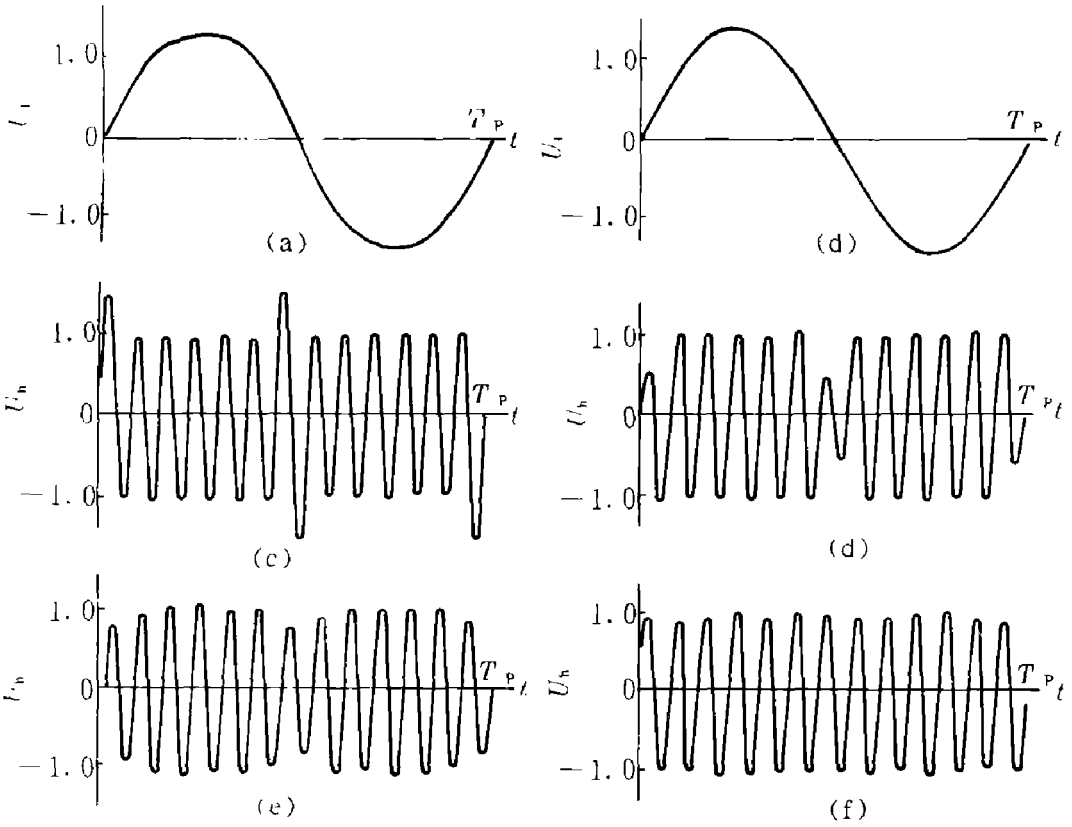

Fig. 8 Voltages at low-and high frequency in dual-frequency receiver, shown in a filtered type of waveforms with varying parameters($k_s = 0.2$)
(a)— $\delta\omega_h = \pi$, $Q = 1$; (b)— $\delta\omega_h = \pi$, $Q = 5$; (c)— $\delta\omega_h = 0$, $Q = 1$;
(d)— $\delta\omega_h = \pi$, $Q = 1$; (e)— $\delta\omega_h = \pi$, $Q = 3$; (f)— $\delta\omega_h = \pi$, $Q = 5$

calculated PFE (PFE_c) and the measured PFE (PFE_m) is not greater than 1% when PFE is less than 30%. The relative error of the average of $\varepsilon = (PFE_m - PFE_c)/PFE_c$ is − 3.36%, which is very stable when anomaly ranges from a very small percentage to 54.5%. This set of results show clearly that dual- frequency IP method matches the conventional variable frequency method in discovering anomaly.

The field measurements also confirmed the above results. Fig. 9 is a practice example made over an antimony mine in Ganshu province, China. The ore mainly consists of antimonite; pyrite and marcasite are common. The ore body is in limestone and is controlled by fractures. For comparison, dual-frequency method, conventional variable frequency method and time domain (TD) IP measurements have been made over the mine. The results show that the three display notable anomalies over the ore body and have similar shapes, except for different

Table 1 Data of PFE_c, PFE_m, ε and the absolute error

PFE_c/%	3.1	5.9	11.7	13.9	16.4
PFE_m/%	3.0	5.7	11.3	13.5	15.8
ε%	−3.5	−3.4	−3.4	−2.9	−3.7
error/%	−0.1	−0.2	−0.4	−0.4	−0.6
PFE_c/%	21.6	24.3	30.5	40.2	47.3	54.5
PEE_m/%	20.9	23.5	29.5	38.8	45.7	52.6
ε%	−3.3	−3.3	−3.3	−3.5	−3.4	−3.5
error/%	−0.7	−0.8	−1.0	−1.4	−1.6	−1.9

absolute values.

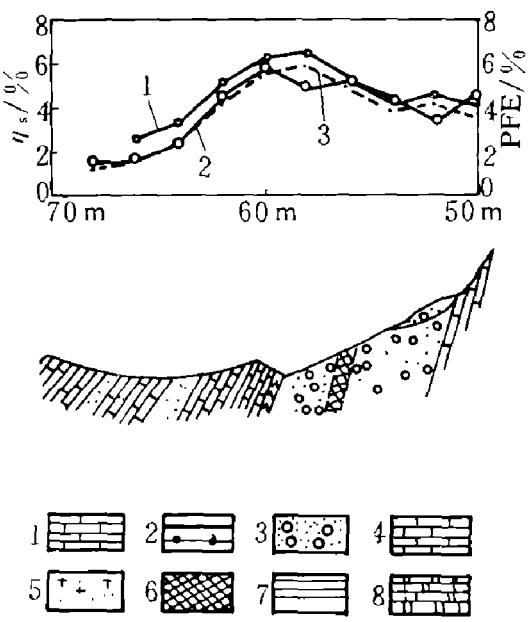

Fig. 9 Comparison of IP profiles

1—PFE measured with dual frequency IP equipment; 2—PFE measured with variable frequency equipment; 3—Chargeability η_s

1—limestone; 2—calcium callys; 3—fractured zone; 4—marbled limestone; 5—halleflinta vein; 6—antimony ore zone; 7—callys; 8—brecciated limestone

5 CONCLUSIONS

(1) Two rectangular currents forming dual-frequency current must be coherent;

(2) Different dual-frequency current waveforms are equivalent in the ability to show IP anomaly;

(3) The effect of current variation on dual-frequency method measurements is much smaller than on conventional variable frequency method. And if power valtage variation is at slow rate, unstabilized current can be used;

(4) Dual-frequency IP method can match variable frequency method and time domain IP method not only in physical principle, but also in the ability of discovering IP anomalies;

Because of its advantages such as fast measuring speed, strong anti-interference ability, and no need of stabilized current, the dual-frequency technique is more applicable to large area reconnaissances.

REFERENCES

1 Wait, J R. In: wait, J R(ed). Overvoltage Research and Geophysical Applications. London: Pergamon Press, 1959, 29—49.

2 Zonge, K L; Wynn, J C. Geophysics, 1975, 10(5): 851—864.

3 Pelton, W H; Ward, S H; Hallof, P G; Sill, W R; Nelson, P H. Geophysics, 1978, 43 (3): 588—609.

4 He Jishan. Journal of Central-South Institute of Mining and Metallurgy, 1978, (2): 1—20.